Enzymatic E-colicins Bind to Their Target Receptor BtuB by Presentation of a Small Binding Epitope on a Coiled-coil Scaffold*

Arun K. Mohanty‡, Christopher M. Bishop§, Thomas C. Bishop¶, William C. Wimley§, and Michael C. Wiener‡∥

From the ‡Department of Molecular Physiology and Biological Physics, University of Virginia, Charlottesville, Virginia 22908-0736, the §Department of Biochemistry, Tulane University Health Sciences Center, New Orleans, Louisiana 70112, and ¶Environmental Health Sciences, Tulane University Health Sciences Center, New Orleans, Louisiana 70112 and the Division of Pharmaceutical Sciences, Xavier University of New Orleans, New Orleans, Louisiana 70125

Toxins and viruses often initiate their attacks by binding to specific proteins on the surfaces of target cells. Bacterial toxins (*e.g.* bacteriocins) and viruses (bacteriophages) targeting Gram-negative bacteria typically bind to outer membrane proteins. Bacterial E-colicins target *Escherichia coli* by binding to the outer membrane cobalamin transporter BtuB. Colicins are tripartite molecules possessing receptor-binding, translocation, and toxin domains connected by long coiled-coil α-helices. Surprisingly, the crystal structure of colicin E3 does not possess a recognizable globular fold in its receptor-binding domain. We hypothesized that the binding epitope of enzymatic E-colicins is a short loop connecting the two α-helices that comprise the coiled-coil region and that this flanking coiled-coil region serves to present the loop in a binding-capable conformation. To test this hypothesis, we designed and synthesized a 34-residue peptide (E-peptide-1) corresponding to residues Ala^{366}–Arg^{399} of the helix-loop-helix region of colicin E3. Cysteines placed near the ends of the peptide (I372C and A393C) enabled crosslinking for reduction of conformational entropy and formation of a peptide structure that would present the loop epitope. A fluorescent analog was also made for characterization of binding by measurement of fluorescence polarization. Our analysis shows the following. (i) E-peptide-1 is predominantly random coil in aqueous solution, but disulfide bond formation increases its α-helical content in both aqueous buffer and solvents that promote helix formation. (ii) Fluorescein-labeled E-peptide-1 binds to purified BtuB in a calcium-dependent manner with a K_d of 43.6 ± 4.9 nM or 2370 ± 670 nM in the presence or absence of calcium, respectively. (iii) In the presence of calcium, cyanocobalamin (CN-Cbl) displaces E-peptide-1 with a nanomolar inhibition constant (K_i = 78.9 ± 5.6 nM). We conclude that the BtuB binding sites for cobalamins and enzymatic E-colicins are overlapping but inequivalent and that the distal loop and (possibly) the short α-helical flanking regions are sufficient for high affinity binding.

A critical first step for the action of many toxins and viruses is binding to proteins or other molecules at the external surface of the target cell. Examples of this process for eukaryotic targets include bacterial toxins and virulence factors that can bind to integrins or other eukaryotic receptors (1), as well as the human immunodeficiency virus that utilizes chemokine receptors (2) and the CD4 surface glycoprotein (3) as co-receptors. This process also occurs in the microbial world, with bacterial toxins (*e.g.* bacteriocins) and bacterial viruses (bacteriophages) binding to surface proteins of susceptible bacteria. Colicins are bacteriocins produced by and active against strains of *Escherichia coli* and closely related bacteria (4–7). Colicins bind to outer membrane proteins such as porins and transporters for cobalamins, siderophores, and nucleosides (4–7). E-colicins, a group of nine closely related colicins called ColE1–9,[1] bind to the *E. coli* outer membrane cobalamin transporter BtuB (8). The structure of BtuB (9) consists of a 22-stranded β-barrel with an amino-terminal hatch domain (Fig. 1, *a* and *b*). Cyanocobalamin (vitamin B$_{12}$, CN-Cbl), a common substrate for BtuB, acts as an inhibitor for E-colicin binding and activity *in vivo* (10, 11). The E-colicins belong to one of the following three cytotoxic classes: (i) membrane depolarizing (or pore forming) colicins such as ColE1; (ii) DNases such as ColE2, ColE7, ColE8, and ColE9; and (iii) RNases such as ColE3, ColE4, ColE5, and ColE6 (7). The enzymatic colicins, ColE2–9, are nearly identical in sequence except for the domains that encode their enzymatic activity.

The lethal action of colicins is executed by three consecutive stages that involve the following: (i) binding to an outer-membrane receptor protein; (ii) transport across the cell envelope; and (iii) biochemical interaction with its target in the cell. These three steps are mediated by three separate parts of the protein, namely a receptor-binding (R) domain located in the central part of the primary sequence, an N-terminal translocation (T) domain, and a carboxyl-terminal catalytic or channel-forming (C) domain, respectively. These domains are linked by long α-helices that form a coiled-coil region. The first intact colicin structure, colicin Ia (12), illustrates clearly this tripartite architecture (Fig. 1*c*). The first (and to date, only) intact E-colicin structure, colicin E3 (13), lacks a clearly identifiable globular R domain (Fig. 1*d*). Where is the R domain in enzymatic E-colicins? The two long α-helices forming the coiled-coil region of ColE3 are linked by a short, seven-residue "hairpin" (Ala^{379}–Gly^{385}), and Soelaiman *et al.* (13) predicted that this loop binds to BtuB. Prior to the elucidation of the ColE3 structure, analysis of amino- and carboxyl-terminal deletion con-

∥ To whom correspondence should be addressed: Dept. of Molecular Physiology and Biological Physics, University of Virginia, PO Box 800736, Charlottesville, VA 22908-0736. Tel.: 434-243-2731; E-mail: mwiener@virginia.edu.

[1] The abbreviations used are: ColE1–9, E-colicin 1–9 (ColE1, ColE2, etc.); CN-Cbl, cyanocobalamin; R domain, receptor-binding domain.
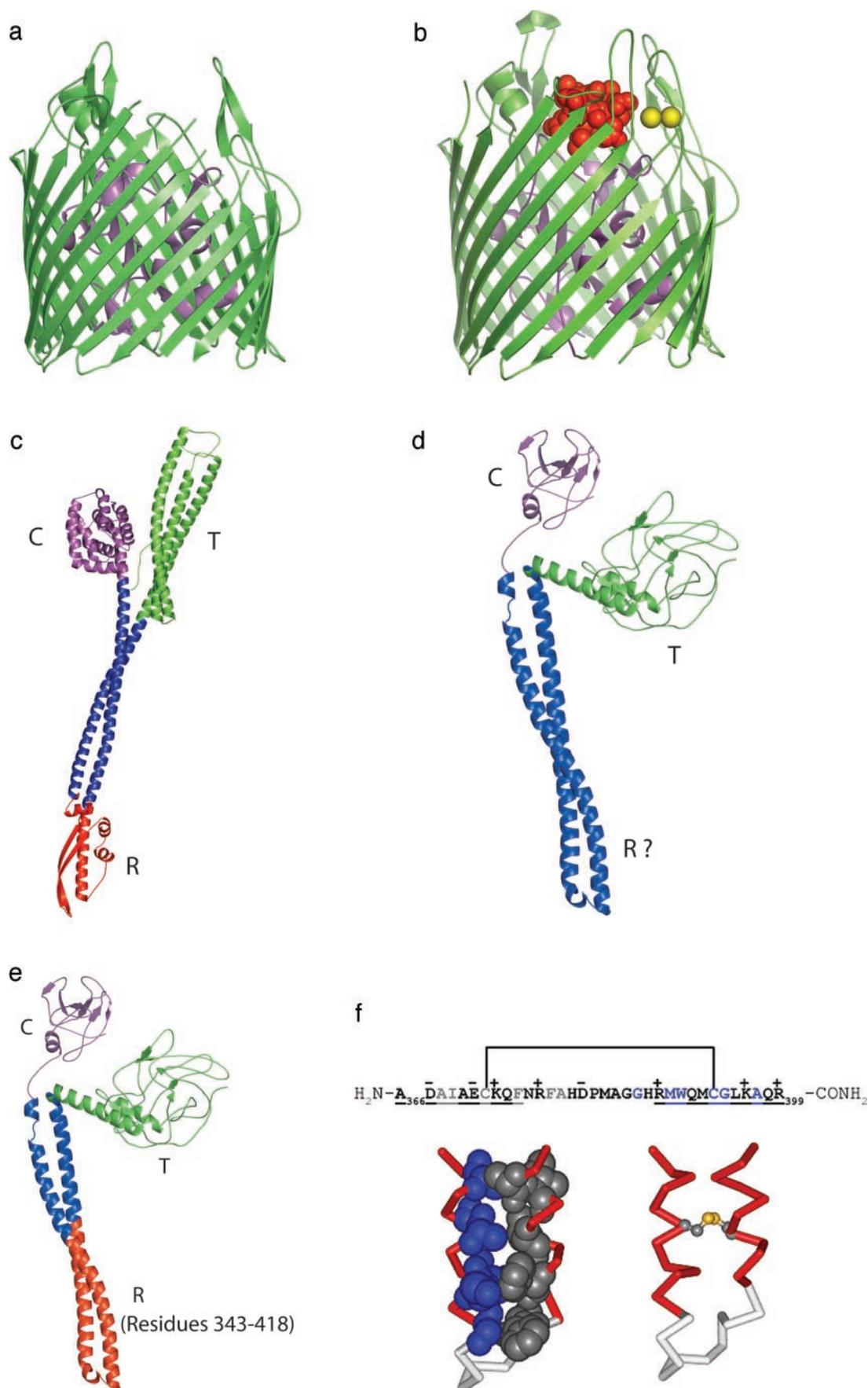
E-colicin Binding to BtuB

FIG. 1. **Structures of BtuB and Colicins Ia and E3.** *a*, Apo-BtuB (Protein Data Bank number 1NQE; Ref. 9) displaying hatch (*magenta*) and barrel (*green*) domains. *b*, ternary complex of BtuB (Protein Data Bank number 1NQH; Ref. 9) displaying bound CN-Cbl (*red*) and calcium ions (*yellow*). *c*, colicin Ia (Protein Data Bank number 1CII; Ref. 12) illustrating the tripartite architecture of colicins. Translocation (*T*), receptor-binding (*R*), and catalytic (*C*) domains are shown in *green*, *red*, and *magenta*, respectively. The coiled-coil region that connects these domains is

structs of ColE9 localized E-colicin R domain properties to a 76-residue region (Fig. 1*e*); this polypeptide bound specifically to BtuB and inhibited the growth of a CN-Cbl-dependent strain of *E. coli* (14). Subsequent solution NMR studies of this construct, interpreted in the context of the ColE3 structure, indicate that it is a helical hairpin structure with multiple conformers in slow exchange and that the connecting loop is flexible (15). Other helix-loop-helix ColE3 domain constructs, 60–135 residues in length, have also been shown to bind specifically to BtuB (16, 17). We hypothesized that the essential binding epitope of the enzymatic E-colicins is this short connecting loop, and the coiled-coil region functions to present this loop in a conformation that is binding competent. Therefore, much of this coiled-coil should be dispensable. We used structure-based design and then synthesized and characterized a 34-residue peptide of ColE3 (E-peptide-1, Fig. 1*f*). E-peptide-1 binds with high affinity to purified BtuB, thus supporting the idea that the coiled-coil is primarily a scaffold for epitope presentation. The calcium-dependence of E-peptide-1 binding and its competitive displacement by the CN-Cbl suggest that enzymatic E-colicins and the cobalamin substrates of BtuB possess overlapping but inequivalent binding sites.

EXPERIMENTAL PROCEDURES

Peptide Design—The design of E-peptide-1 started with the ColE3 wild type sequence Ala[366]–Arg[399]. Because cyclization can significantly stabilize peptide tertiary structure (18, 19) by decreasing conformational entropy, a disulfide linkage was engineered. Using SwissPDB Viewer (20) with the ColE3 structure as a template, all possible Cys-Cys disulfides were modeled and energy minimized. Six possible disulfide cross-linked peptides that had cysteine residues with normal C_α-C_β-S and C_β-S-S dihedral angles of 110° and 105°, respectively, and normal C-S and S-S distances of 1.55 Å and 1.90 Å, respectively, were identified. These variants all had backbone tertiary structures that were very similar to the native structure, with maximum atomic deviations of ~0.3 Å in the vicinity of the disulfide bond. From these six possibilities, F378C/W390C, I372C/A393C, D381C/H387C, A368C/A397C, F375C/W390C, and F375C/M389C, two (I372C/A393C and A368C/A397C) were nearly isovolumetric and did not alter the total charge of the sequence. From among these two, I372C/A393C was selected because it is closest to the native hydrophobicity (21) and because it is located in the middle of the coiled-coil where the crosslink is expected to have the greatest stabilizing effect (Fig. 1*f*).

Peptide Synthesis and Purification—E-peptide-1 was synthesized by *N*-(9-fluorenyl)methoxycarbonyl (Fmoc) chemistry (22, 23) using an Applied Biosystems Pioneer synthesizer. The solid support was PEG-PS-PAL resin (Applied Biosystems, Foster City, CA) with a loading of 0.25 mmol/g. The groups pbf and Trt (22) were used for the critical side-chain protection of Arg and Cys, respectively. After observing large amounts of pbf adducts on Trp in a preliminary synthesis, Boc-protection of the Trp side-chain was used to prevent its recurrence. Protecting groups were cleaved efficiently using a 2-h treatment with 90% trifluoroacetic acid, 5% thioanisole, 3% ethanedithiol, and 2% anisole. Cleavage was performed in a dark N_2 atmosphere with the first 15 min of cleavage carried out at 0 °C and the remainder at room temperature. Cleaved peptide was filtered from the resin, dried immediately under a stream of nitrogen, and then lyophilized repeatedly from glacial acetic acid. Lyophilized E-peptide-1 was reduced with aqueous dithiothreitol and then partially purified with PolyCat A cation exchange resin (Western Analytical, Murietta, CA). Peptide was bound to the PolyCat A resin, and then the dithiothreitol and other contaminants were removed by extensively washing the resin with water and isopropanol. Finally,

the pure peptide was eluted from the resin with 45% acetic acid. Mass spectrometry on this material gave the mass of 3877 ± 2 Da (predicted mass, 3876.4 Da). There were no major contaminants and no evidence that the acid-labile Asp-Pro bond (24) had been cleaved. Reduced E-peptide-1, which is highly soluble in water, was oxidized at 20 mg/ml for 24 h in 10% Me_2SO/water (25). Oxidized peptide was analyzed with mass spectrometry, and no evidence of crosslinked dimers or higher oligomers was found. We verified that the peptides were cyclized by cleaving the Asp-Pro bond at residue 16 in formic acid (24) and then using high performance liquid chromatography and mass spectrometry to show that the resulting single species was separated into two peptide species of the expected masses of 1838 and 2058 Da only upon disulfide bond reduction. Final purification of the cyclized E-peptide-1 peptide was done with C18 reverse phase high performance liquid chromatography. Linear E-peptide-1 was made by reduction with dithiothreitol and *S*-carboxyamidomethylation with iodoacetamide. Fluorescein-labeled E-peptide-1 was made by labeling the peptide's amino terminus with fluorescein succinimidyl ester (Molecular Probes, Eugene, OR) while the peptide was still attached to the solid support and while its lysine side-chains were still protected. Cleavage, deprotection, oxidation, and purification of the labeled peptide were done as described above.

CD Spectroscopy—Circular dichroism spectra of oxidized and reduced E-peptide-1 peptide were collected from samples in a 0.1-mm path length quartz cuvette using a circular dichroism spectrometer (JASCO Model 810). Spectra were collected from 300 to 180 nm with 1-nm step size, 1-nm bandwidth, and at a rate of 10 nm/min. Spectra were recorded at 20–40 μM peptide in distilled water or water that contained 30 or 60% trifluoroethanol, a helix-promoting solvent (26)

Fluorescence Polarization Binding Assays—BtuB was expressed and purified as described previously (27). The peak fractions after the final anion exchange purification step were passed over PD-10 desalting columns (Amersham Biosciences) into assay buffer (30 mM Tris-Cl, pH 8.0, and 0.6% *n*-octyl tetraoxyethylene (C_8E_4; Anatrace, Maumee, OH)). This assay buffer contains 1.6 μM free calcium as determined by fluorescence-ratio analysis of Fura-2 (Molecular Probes). BtuB concentration was determined by measurement of A_{280} and use of an extinction coefficient of 198,329 M^{-1} cm^{-1} as determined by quantitative amino acid analysis (W. M. Keck Facility, Yale University, New Haven, CT). E-peptide-1 concentration was determined in a similar way using an extinction coefficient $\epsilon_{280} = 7,253$ M^{-1} cm^{-1}. Fluorescein-labeled E-peptide-1 concentration was measured by absorbance spectroscopy using an extinction coefficient $\epsilon_{498} = 88,000$ M^{-1} cm^{-1} and used at a concentration of 5–6 nM in the assays. The concentration of CN-Cbl was estimated by absorbance using $A_{361(1 cm)}^{(1\%)} = 204$ (28). Fluorescence polarization (*P*) at 20 °C was measured with a Beacon 2000 fluorescence polarization instrument (PanVera, Madison, WI) with filters at 490 nm (excitation) and 530 nm (emission). Fluorescence polarization (*P*) values were converted to anisotropy (*A*) values by the equation $A = 2P/(3 - P)$; anisotropy of the free peptide was typically ~0.1. Data were fitted using KaleidaGraph (Synergy Software, Reading, PA) to the equation $A = A_f + ((A_b - A_f)[protein]/(K_d + [protein]))$, with A_f and A_b representing the anisotropy of the free and bound peptides, respectively. Competitive binding studies were performed using BtuB and fluorescein-labeled E-peptide-1 concentrations at which >90% of the peptide was bound to BtuB. Competing ligands (CN-Cbl or unlabeled E-peptide-1) were added, and the change in *P* with ligand titration was measured. Anisotropy data were fitted to the equation $A = A_f + ((A_b - A_f)[I]/(IC_{50} + [I]))$, where A_f, A_b, and I are anisotropy of free competing ligands, anisotropy of the bound competing ligands, and total concentration of the competing ligands, respectively. The IC_{50} value of each competing ligand was converted to K_i by the equation $K_i = (0.5 B)(IC_{50})(K_d)/((L_T R_T) + 0.5B(-R_T - L_T + 0.5B - K_d))$, where B, IC_{50}, L_T, and R_T are bound fluorescent ligand, concentration of competitor at 50% inhibition, total fluorescent ligand, and total protein concentration respectively (29).

shown in *blue*. *d*, the Colicin E3 (Protein Data Bank number 1JCH; Ref. 13) structure displaying the T (*green*) and C (*magenta*) domains. The immunity protein Im3 that is bound to ColE3 in the structure has been omitted for clarity. Unlike colicin Ia, a globular receptor-binding domain is not apparent. *e*, the 76-residue sequence (343–418) of Colicin E9 that displayed BtuB-binding function (Ref. 14) is mapped (in *red*) onto the ColE3 structure. These regions are at least 95% identical in all enzymatic E-colicins for which sequences are available. *f*, sequence and design of E-peptide-1. *Top*, sequence of E-peptide-1, corresponding to Ala[366]–Arg[399] in ColE3. In the synthetic peptide, Ile[372] and Ala[393] have been replaced with cysteines to make the indicated intramolecular disulfide crosslink. Residues that are in the helical coiled-coil in the native protein are *underlined*, and the residues in the extensive hydrophobic interface of the coiled-coils are highlighted in *gray* (amino-terminal helix) and *blue* (carboxyl-terminal helix). *Bottom left*, E-peptide-1 as mapped onto the ColE3 structure. A backbone trace in *red* indicates residues with helical conformation. Hydrophobic residues in the coiled-coil interface are shown in space-filling mode using the same *gray* and *blue* color code as above in the sequence. *Bottom right*, the location of the disulfide linkage in the context of the native structure.
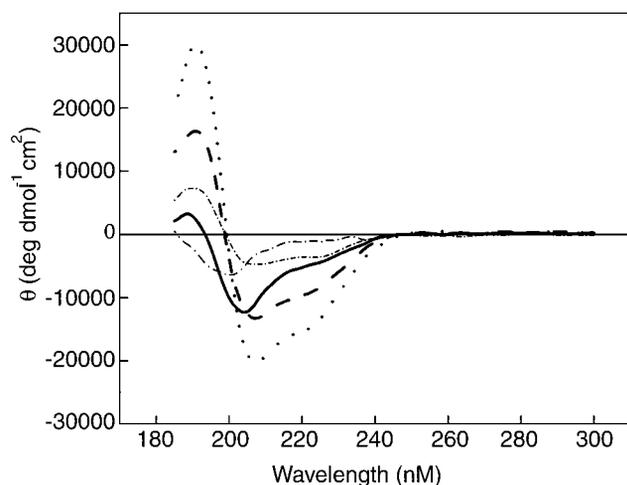
FIG. 2. **Circular dichroism spectra of cyclic, oxidized E-peptide-1, and linear, reduced E-peptide-1.** *Long dash-dot*, reduced peptide in water; *short dash-dot*, reduced peptide in 60% trifluoroethanol; *solid line*, oxidized peptide in water; *dashed line*, oxidized peptide in 30% trifluoroethanol; *dotted line*, oxidized peptide in 60% trifluoroethanol. The oxidized E-peptide-1 is more structured than the reduced peptide under all conditions.
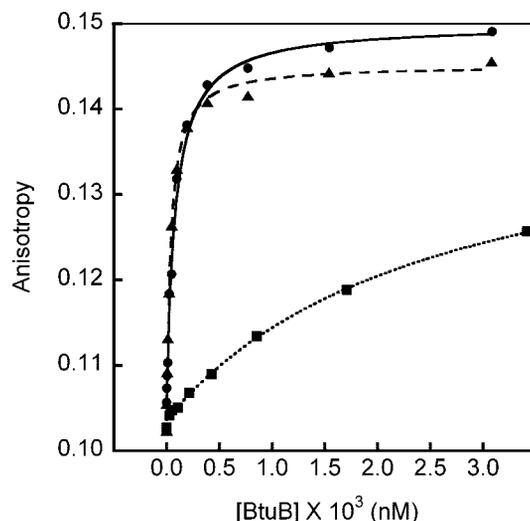

FIG. 3. **Binding isotherms of purified BtuB with fluorescein-labeled E-peptide-1.** Curves represent the best fit to the data as described under "Experimental Procedures." Binding assays were performed in the standard assay buffer without added extra calcium (*solid line* with ●), the buffer with 20 μM CaCl$_2$ added (*broken line* with ▲), and the buffer with 100 μM EGTA added (*dotted line* with ■).

RESULTS

The α-Helical Content of E-peptide-1 Increases with Disulfide Bond Formation—CD spectra are shown in Fig. 2. Reduced, linear E-peptide-1 is random coil with a broad minimum centered at 200 nM and essentially zero ellipticity in the α-helical region between 210 and 225 nm (30). Oxidized disulfide-linked E-peptide-1 has more ordered secondary structure in water as seen by a shift in the minimum up to 204 nm, a crossover to a positive peak at 190 nm, and measurable ellipticity in the α-helical region. Disulfide-linked E-peptide-1 contains about 10% helix in water based upon the mean residue ellipticity at 222 nm. In the presence of 60% trifluoroethanol, a helix-promoting solvent, the helical content of disulfide-linked E-peptide-1 increases to ~40%, whereas reduced E-peptide-1 remains low at ~10%.

E-peptide-1 Binds to BtuB with a Calcium-dependent Nanomolar Affinity—Fluorescence polarization binding isotherms of fluorescein-labeled E-peptide-1 are shown in Fig. 3, and equilibrium binding constants K_d are listed in Table I. A single site binding model adequately fits the observed data. In the presence of 100 μM EGTA, fluorescein-labeled E-peptide-1 binds with only micromolar affinity ($K_d = 2370 \pm 670$ nM; $n = 4$). Omission of EGTA and the addition of 20 μM CaCl$_2$ to the assay buffer increases binding affinity dramatically by >50-fold ($K_d = 43.6 \pm 4.9$ nM; $n = 4$). The affinity decreases slightly, $K_d = 73.9 \pm 8.3$ nM ($n = 4$) in the standard assay buffer that contains 1.6 μM free calcium.

CN-Cbl, a Substrate for BtuB, Displaces Bound E-peptide-1 in the Presence of Calcium—The BtuB substrate CN-Cbl is able to displace competitively bound fluorescein-labeled E-peptide-1. Fluorescence polarization competitive binding isotherms are shown in Fig. 4a, and equilibrium inhibition constants K_i are listed in Table I. In the presence of 100 μM EGTA, CN-Cbl up to a maximum assay concentration of 66 μM is unable to displace bound fluorescein-labeled E-peptide-1. A single site competitive binding model adequately fits the other observed data. The omission of EGTA and the addition of 20 μM CaCl$_2$ to the assay buffer enables CN-Cbl to now displace bound fluorescein-labeled E-peptide-1 with a nanomolar inhibition constant ($K_i = 78.9 \pm 5.6$ nM; $n = 4$). In the standard assay buffer that contains 1.6 μM free calcium, K_i increases slightly to 90.4 ± 10.4 nM ($n = 3$). The difference between these two values is not statistically significant. The ability of unla-

beled E-peptide-1 to displace fluorescein-labeled E-peptide-1 was included as a positive control and to determine the effect, if any, of the fluorescent moiety upon binding (Fig. 4b). In contrast to competition by CN-Cbl, unlabeled E-peptide is able to displace bound fluorescein-labeled E-peptide-1 in the presence of 100 μM EGTA, although with a micromolar inhibition constant ($K_i = 2620 \pm 780$ nM; $n = 2$). Omission of EGTA and addition of 20 μM CaCl$_2$ to the assay buffer increases inhibition dramatically by >50-fold ($K_i = 49.9 \pm 21.4$ nM; $n = 4$). The inhibition constant increases slightly ($K_i = 99.5 \pm 19.8$ nM; $n = 3$), in the standard assay buffer.

DISCUSSION

We successfully used the crystal structure of ColE3 (13) as a template for design and construction of a minimal receptor-binding domain, E-peptide-1, that binds to the outer membrane cobalamin transporter BtuB with nanomolar affinity. This result supports the hypothesis that the primary binding epitope of enzymatic E-colicins is a short loop connecting the two α-helices that comprise the coiled-coil region and (possibly) includes relatively short segments of this flanking coiled-coil region. In the colicin binding event, the main function of the coiled-coil region is to form a scaffold for presentation of the loop epitope in a binding-competent conformation. Two peptide/protein design criteria were applied. First, minimizing the length of the peptide while maintaining at least two to three turns of each of the α-helices flanking the putative loop epitope. Second, substituting two cysteines into the wild type peptide sequence to enable formation of a disulfide crosslink for minimization of conformational entropy. Based on these criteria, we selected the 34-residue peptide E-peptide-1 (corresponding to Ala[366]–Arg[399], with cysteine substitutions I372C and A393C (Fig. 1f). The E-peptide-1 sequence, in the context of the ColE3 crystal structure, is ~75% helical. In contrast, disulfide-linked E-peptide-1 is only ~10% helical in aqueous solvents. However, the helical content increases to ~40% in helix-promoting solvents. Critically, the helical content of reduced and *S*-carboxyamidomethylated E-peptide-1, near zero in water, did not change in helix-promoting solvents. Although synthetic E-peptide-1 possesses less secondary structure than when its sequence is present within the entire ColE3 protein, the isolated peptide can form α-helical structure under the appropriate

TABLE I

Equilibrium binding constants of fluorescein-labeled E-peptide-1 and competitive inhibitors CN-Cbl and E-peptide-1

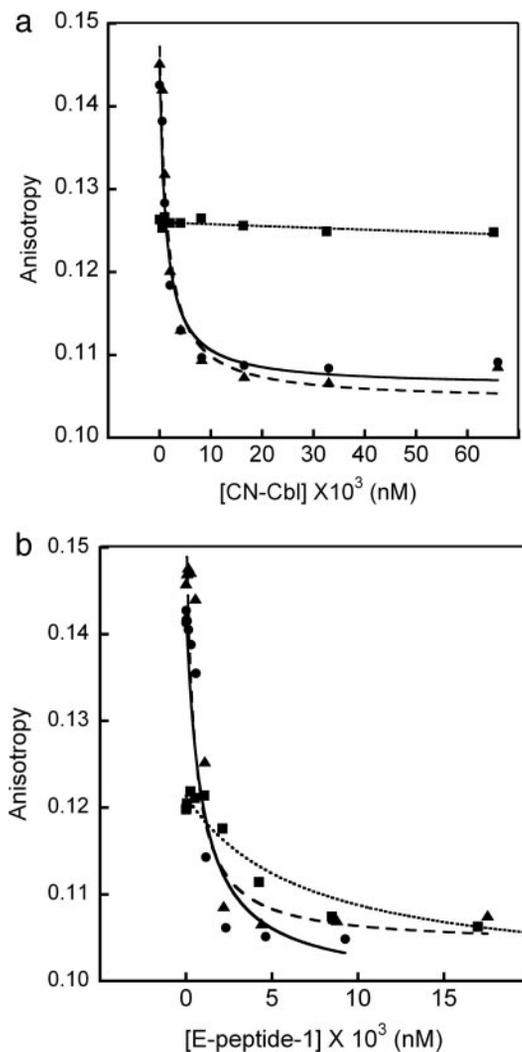| Buffer	K_d (Fluorescein-labeled E-peptide-1)	K_i (CN-Cbl)	K_i (E-peptide-1)
	nM	nM	nM
Standard assay buffer (1.6 μM CaCl$_2$)	73.9 ± 8.3 ($n = 4$)	90.4 ± 10.4 ($n = 3$)	99.5 ± 19.8 ($n = 3$)
Standard assay buffer + 20 μM CaCl$_2$	43.6 ± 4.9 ($n = 4$)	78.9 ± 5.6 ($n = 4$)	49.9 ± 21.4 ($n = 4$)
Standard assay buffer + 100 μM EGTA	2370 ± 670 ($n = 4$)	No binding observed ($n = 2$)	2620 ± 780 ($n = 2$)

FIG. 4. **Competition binding isotherms of CN-Cbl (*a*) and unlabeled E-peptide-1 (*b*) against fluorescein-labeled E-peptide-1 bound to BtuB**. Binding assays were performed in the buffer without added extra calcium (*solid line* with ●), the buffer with 20 μM CaCl$_2$ added (broken lines with ▲), and the buffer with 100 μM EGTA (*dotted line* with ■).

environmental conditions; these conditions may include an induced-fit mechanism upon binding to BtuB. Importantly, this structuring is significantly enhanced, *i.e.* $\Delta G_{structure}$ is more favorable, when the disulfide crosslink is in place.

Calcium is necessary for high affinity binding of CN-Cbl to BtuB, with a 50–100-fold decrease in affinity when calcium is depleted (31). Crystal structures of BtuB show that the addition of calcium induces an ordering of extracellular loops of the β-barrel and indicate a direct structural role for these ions in high affinity CN-Cbl binding (9). We observe an analogous calcium-dependent binding of E-peptide-1. Binding of fluorescein-labeled E-peptide-1 in the absence of calcium is ~50-fold weaker than in the presence of 20 μM calcium; competitive displacement of fluorescein-labeled E-peptide-1 by E-peptide-1

is ~50-fold less effective (Table I). The apparent K_d of calcium binding to BtuB in isolated outer membranes is 30 nM (31); therefore, 20 μM calcium is saturating. In competition binding experiments, CN-Cbl displaces E-peptide-1 with a nanomolar inhibition constant in the presence of calcium but cannot displace the peptide in calcium-depleted buffers. These two observations, a calcium dependence of E-peptide binding (like that of CN-Cbl binding) and displacement of E-peptide by CN-Cbl, indicate that the binding sites of cobalamins and enzymatic E-colicins are similar. However, the inhibition constant ($K_i = 78.9 \pm 5.6$ nM; $n = 4$) for CN-Cbl to displace fluorescein-labeled E-peptide-1 from BtuB is 50–250-fold larger than reported K_d values for binding of CN-Cbl to BtuB (27, 31). This result, that $K_i \gg K_d$ for CN-Cbl interaction with BtuB, implies that the binding sites for cobalamins and enzymatic E-colicins overlap but are not equivalent. Chemical modification experiments suggest that the ion channel-forming E-colicin, ColE1, binds differently to BtuB than the enzymatic E-colicins ColE2 and ColE3 (32). This may reflect the different killing mechanisms of these two types of colicins. Following the binding event, enzymatic E-colicins are transported across both the outer and inner membranes in a process still rather poorly understood (33).

REFERENCES

1. Knodel, L. A., Celli, J., and Finlay, B. B. (2001) *Nat. Rev. Mol. Cell Biol.* **2,** 578–588
2. Dragic, T., Litwin, V., Allaway, G. P., Martin, S. R., Huang, Y., Nagashima, K. A., Cayanan, C., Maddon, P. J., Koup, R. A., Moore, J. P., and Paxton, W. A. (1996) *Nature* **381,** 667–673
3. Lifson, J. D., Feinberg, M. B., Reyes, G. R., Rabin, L., Banapour, B., Chakrabarti, S., Moss, B., Wong-Staal, F., Steimer, K. S., and Engelman, E. G. (1986) *Nature* **323,** 725–728
4. Lazdunski, C. J., Bouveret, E., Rigal, A., Journet, L., Lloubes, R., and Benedetti, H. (1998) *J. Bacteriol.* **180,** 4993–5002
5. Cramer, W. A., Heymann, J. B., Schendel, S. L., Deriy, B. N., Cohen, F. S., Elkins, P. A., and Stauffacher, C. V. (1995) *Annu. Rev. Biophys. Biomol. Struct.* **24,** 611–641
6. Braun, V., Pilsl, H., and Gross, P. (1994) *Arch. Microbiol.* **161,** 199–206
7. James, R., Kleanthous, C., and Moore, G. R. (1996) *Microbiology* **142,** 1569–1580
8. Heller, K., Mann, B. J., and Kadner, R. J. (1985) *J. Bacteriol.* **161,** 896–903
9. Chimento, D. P., Mohanty, A. K., Kadner, R. J., and Wiener, M. C. (2003) *Nat. Struct. Biol.* **10,** 394–401
10. Di Masi, D. R., White, J. C., Schnaitman, C. A., and Bradbeer, C. (1973) *J. Bacteriol.* **115,** 506–513
11. Cavard, D. (1994) *FEMS Microbiol. Lett.* **116,** 37–42
12. Wiener, M., Freymann, D., Ghosh, P., and Stroud, R. M. (1997) *Nature* **385,** 461–464
13. Soelaiman, S., Jakes, K., Wu, N., Li, C., and Shoham, M. (2001) *Mol. Cell* **8,** 1053–1062
14. Penfold, C. N., Garinot-Schneider, C., Hemmings, A. M., Moore, G. R., Kleanthous, C., and James, R. (2000) *Mol. Microbiol.* **38,** 639–649
15. Boetzel, R., Collins, E. S., Clayden, N. J., Kleanthous, C., James, R., and Moore, G. R. (2003) *Faraday Discuss.* **122,** 145–162
16. Zakharov, S. D., Bano, S., Zhalnina, M., and Cramer, W. A. (2003) *Biophys. J.* **84,** 324a (abstr.)
17. Bano, S., Zakharov, S. D., Zhalnina, M., Lindeberg, M., Shoham, M., and Cramer, W. A. (2002) *Biophys. J.* **82,** 554a (abstr.)
18. Hocart, S. J., Jain, R., Murphy, W. A., Taylor, J. E., and Coy, D. H. (1999) *J. Med. Chem.* **42,** 1863–1871
19. Tam, J. P., Wu, C., and Yang, J. L. (2000) *Eur. J. Biochem.* **267,** 3289–3300
20. Guex, N., and Peitsch, M. C. (1997) *Electrophoresis* **18,** 2714–2723
21. Wimley, W. C., Creamer, T. P., and White, S. H. (1996) *Biochemistry* **35,** 5109–5124
22. Grant, G. A. (1992) *Synthetic Peptides: A User's Guide*, W. H. Freeman and Co., New York

23. Atherton E., and Sheppard, R. C. (1989) *Solid Phase Peptide Synthesis*, IRL Press, Oxford
24. Piszkiewicz, D., Landon, M., and Smith, E. L. (1970) *Biochem. Biophys. Res. Comm.* **40,** 1173–1178
25. Tam, J., Wu, C.-R., Liu, W., and Zhang, J.-W. (1991) *J. Am. Chem. Soc.* **113,** 6657–6662
26. Nelson, J. W., and Kallenbach, N. R. (1986) *Proteins* **1,** 211–217
27. Chimento, D. P., Mohanty, A. K., Kadner, R. J., and Wiener, M. C. (2003) *Acta Crystallogr. Sect. D Biol. Crystallogr.* **59,** 509–511
28. Budavari, S. (1996) *The Merck Index: An Encyclopedia of Chemicals, Drugs and Biologicals*, 12th Ed., p. 1710, Whitehouse Station, NJ
29. Kenakin, T. (1997) *Pharmacological Analysis of Drug/Receptor Interaction*, 3rd Ed., pp. 242–288, Lippincott-Raven, New York
30. Johnson, W. C., Jr. (1990) *Proteins* **7,** 205–214
31. Bradbeer, C., Reynolds, P. R., Bauler, G. M., and Fernandez, M. T. (1986) *J. Biol. Chem.* **261,** 2520–2523
32. Šmarda, J., and Macholan, L. (2000) *Folia Microbiol.* **45,** 379–385
33. Cao, Z., and Klebba, P. E. (2002) *Biochimie (Paris)* **84,** 399–412